MOLECULAR AND CELLULAR BIOLOGY, Sept. 2002, p. 6521–6532 Vol. 22, No. 18
0270-7306/02/$04.00+0 DOI: 10.1128/MCB.22.18.6521–6532.2002


# Chk2 Is a Tumor Suppressor That Regulates Apoptosis in both an Ataxia Telangiectasia Mutated (ATM)-Dependent and an ATM-Independent Manner

Atsushi Hirao,[1,2] Alison Cheung,[1] Gordon Duncan,[1] Pierre-Marie Girard,[3] Andrew J. Elia,[1] Andrew Wakeham,[1] Hitoshi Okada,[1] Talin Sarkissian,[1] Jorge A. Wong,[1] Takashi Sakai,[1] Elisa de Stanchina,[4] Robert G. Bristow,[5] Toshio Suda,[2] Scott W. Lowe,[4] Penny A. Jeggo,[3] Stephen J. Elledge,[6] and Tak W. Mak[1]*

*Departments of Medical Biophysics and Immunology, Ontario Cancer Institute, University of Toronto, Toronto, Ontario M5G 2C1,[1] and Department of Radiation Oncology and Department of Medical Biophysics, Ontario Cancer Institute, University of Toronto, Toronto, Ontario M5G 2M9,[5] Canada; Genome Damage and Stability Centre, University of Sussex, Falmer, Sussex BN1 9RR, United Kingdom[3]; Cold Spring Harbor Laboratory, Cold Spring Harbor, New York 11724[4]; Verna and Marrs McLean Department of Biochemistry and Molecular Biology and Department of Molecular and Human Genetics, Howard Hughes Medical Institute, Baylor College of Medicine, Houston, Texas 77030[6]; and The Sakaguchi Laboratory of Developmental Biology, School of Medicine, Keio University, Tokyo 160-8582, Japan[2]*

Received 5 March 2002/Accepted 18 June 2002

**In response to ionizing radiation (IR), the tumor suppressor p53 is stabilized and promotes either cell cycle arrest or apoptosis. Chk2 activated by IR contributes to this stabilization, possibly by direct phosphorylation. Like p53, Chk2 is mutated in patients with Li-Fraumeni syndrome. Since the ataxia telangiectasia mutated (ATM) gene is required for IR-induced activation of Chk2, it has been assumed that ATM and Chk2 act in a linear pathway leading to p53 activation. To clarify the role of Chk2 in tumorigenesis, we generated gene-targeted Chk2-deficient mice. Unlike $ATM^{-/-}$ and $p53^{-/-}$ mice, $Chk2^{-/-}$ mice do not spontaneously develop tumors, although Chk2 does suppress 7,12-dimethylbenzanthracene-induced skin tumors. Tissues from $Chk2^{-/-}$ mice, including those from the thymus, central nervous system, fibroblasts, epidermis, and hair follicles, show significant defects in IR-induced apoptosis or impaired $G_1$/S arrest. Quantitative comparison of the $G_1$/S checkpoint, apoptosis, and expression of p53 proteins in $Chk2^{-/-}$ versus $ATM^{-/-}$ thymocytes suggested that Chk2 can regulate p53-dependent apoptosis in an ATM-independent manner. IR-induced apoptosis was restored in $Chk2^{-/-}$ thymocytes by reintroduction of the wild-type Chk2 gene but not by a Chk2 gene in which the sites phosphorylated by ATM and ataxia telangiectasia and *rad3*$^+$ related (ATR) were mutated to alanine. ATR may thus selectively contribute to p53-mediated apoptosis. These data indicate that distinct pathways regulate the activation of p53 leading to cell cycle arrest or apoptosis.**

DNA damage activates cellular responses that promote DNA repair, arrest the cell cycle, and in some cases, induce apoptosis (56). Cell cycle arrest allows time for the repair of damaged DNA while apoptosis eliminates cells harboring abnormal DNA. It is widely believed that these DNA damage responses are required for the maintenance of genomic stability and prevention of tumor development (20).

The ataxia telangiectasia (A-T) mutated (ATM) gene, which is homologous to the yeast checkpoint gene Tel1, plays a critical role in sensing DNA double strand breaks (DSBs) in mammalian DNA. ATM is a kinase involved in activating the appropriate damage response pathway, leading to either cell cycle arrest or apoptosis, and is therefore a key checkpoint molecule in regulating cell cycle responses to DNA damage (37, 45). Indeed, the majority of phosphorylation events induced by ionizing radiation (IR) are carried out by ATM. Both A-T patients and ATM-deficient mice show defective cell cycle arrest, hypersensitivity to DNA DSBs, and tumor predisposition (4, 21, 52, 53). When cells are damaged by IR, ATM phosphorylates and activates the protein kinase Chk2 (1, 35, 36, 55). Chk2 is a homologue of the Rad53 gene in budding yeast and of the Cds1 gene in fission yeast. Once phosphorylated, activated Chk2 phosphorylates multiple Cdc25 molecules which are thought to inhibit the activation of cyclin-dependent kinases (7, 10, 34). However, in response to damage induced by UV-irradiation or hydroxyurea, Chk2 is phosphorylated in an ATM-independent manner, possibly by A-T and *rad3*$^+$ related (ATR) (35, 46). Notably, ATM, ATR, and Chk2 are each able to phosphorylate the tumor suppressor gene p53 (2, 9, 11, 26, 42, 49).

p53 is the most frequently mutated cancer-associated gene identified to date (29). In response to DNA damage, p53 undergoes phosphorylation and conformational changes which result in increased levels and activity of the protein (23). Increased p53 activity enhances the rate of transcription of numerous target genes (such as p21, Mdm2, GADD45, and Bax) that mediate the plethora of p53-dependent functions (19, 54). These functions include the promotion of apoptosis and the induction of $G_1$ cell cycle arrest. The p53 protein can be mod-

* Corresponding author. Mailing address: Ontario Cancer Institute, University of Toronto, 620 University Ave., Suite 706, Toronto, Ontario M5G 2C1, Canada. Phone: (416) 204-2236. Fax: (416) 204-5300. E-mail: tmak@uhnres.utoronto.ca.

ified by many different protein kinases and acetylases, resulting in modulation of p53 function (39). In particular, the phosphorylation or dephosphorylation of various serine residues can have a significant impact on p53 stability. Recent studies with phospho-specific antibodies have established that serines (Ser) 6, 9, 15, 20, 33, 37, and 46 of p53 are sites of de novo phosphorylation in cells following DNA damage and that phosphorylation of different sites has different effects (2, 9, 12, 25, 38, 43, 44, 47). For example, it has been proposed that the phosphorylation of the N-terminal Ser 15, 33, and 37 residues permits subsequent modification of the distant C-terminal lysine residues of p53 through enhanced recruitment of the coactivator protein p300/CBP/PCAF (28, 41). In contrast, phosphorylation of Ser20 is required for stability of p53 in response to DNA damage (11). Ser20 comprises part of the site used by Mdm2 to bind p53 and target it for ubiquitination, and phosphorylation of Ser20 interferes with Mdm2 binding.

Previous studies have demonstrated that, in response to IR, Ser15 on p53 is phosphorylated by ATM (2, 9), whereas Ser20 is phosphorylated by Chk2 (11, 26, 42). There is abundant evidence that ATM controls p53 stabilization either directly or indirectly via Chk2, and it is also now clear that p53-mediated $G_1$ arrest is suppressed in $ATM^{-/-}$ thymocytes. However, it is more controversial whether ATM is involved in p53-mediated apoptosis of damaged cells. While some laboratories have shown that $ATM^{-/-}$ thymocytes are resistant to IR-induced apoptosis (51, 53), others have found that these cells exhibit normal p53-mediated cell death (3, 21, 24). It appears that the pathways governing p53-dependent cell cycle arrest and apoptosis may be distinct and that ATM plays a major role in regulating only the former.

Previous work on Chk2-deficient thymocytes reconstituted from $Chk2^{-/-}$ embryonic stem (ES) cells in $Rag1^{-/-}$ mice showed that Chk2 contributes to p53 stabilization following exposure to IR (26). We have now created mutant mice in which the Chk2 gene was disrupted through homologous recombination. We report on the phenotype of $Chk2^{-/-}$ mice and compare it to that of $ATM^{-/-}$ mice. Using various $Chk2^{-/-}$ cell types, we show that Chk2 is involved in both ATM-dependent and ATM-independent regulation of IR-induced p53-mediated apoptosis.

## MATERIALS AND METHODS

**Generation of $Chk2^{-/-}$ mice.** To generate $Chk2^{-/-}$ mice, fragments of the murine Chk2 gene were isolated from a mouse 129 genomic library by using the mouse Chk2 cDNA as a probe. The targeting construct was designed to delete the exons encoding the conserved kinase sequence as described previously (26). ES clones heterozygous for the targeted mutation were isolated by drug selection and confirmed by Southern blotting. Two independent heterozygous ES clones were injected into 3.5-day C57BL/6 blastocysts which were subsequently transferred into pseudopregnant foster mothers. Chimeric mice were crossed into C57BL/6 mice to produce heterozygous $Chk2^{+/-}$ mice which were subsequently intercrossed to generate $Chk2^{-/-}$ animals. $p53^{-/-}$ mice were purchased from Taconic. $ATM^{-/-}$ mice were the kind gift of Peter J. McKinnon (St. Jude Children's Research Hospital).

**Apoptosis assays.** To analyze apoptosis in the thymus in vivo, 6- to 8-week-old mice were irradiated with 10 Gy of irradiation from a $^{137}Cs$ source (Gammacell 40) at a dose of 1.0 Gy/min. For apoptosis in the central nervous system (CNS) or skin, mice at day 5 after birth (P5) and P7, respectively, were irradiated with 5 Gy of irradiation. Mice were anesthetized by cooling, and their hearts were perfused with ice-cold saline followed by fixation in ice-cold 4% paraformaldehyde. The brains were removed and fixed for a further 24 to 48 h in 4% paraformaldehyde at 4°C. The thymus and skin from the dorsal area were fixed in 10% buffered formalin overnight at 4°C. Tissue samples were embedded in wax by following standard procedures and sectioned at a thickness of 5 to 7 μm. Apoptosis in thymus, skin, and brain sections was analyzed by the terminal deoxynucleotidyltransferase-mediated dUTP nick end labeling (TUNEL) assay (Boehringer-Mannheim). Sectioned material was prepared for the TUNEL assay by following standard procedures (33). Briefly, sections were deparaffinized and rehydrated through a graded series of ethanol solutions to phosphate-buffered saline. Sections were then subjected to the TUNEL assay. To quantify the apoptosis of thymocytes in vitro, thymocytes were isolated from 5- to 8-week-old mice and irradiated with 1 to 4 Gy of irradiation. Apoptotic cells were detected by flow cytometric analysis with Annexin V and propidium iodide (PI) staining (R&D Systems).

**Cell cycle analysis.** For analysis of $G_1$ arrest in the skin, P7 mice were irradiated with 5 Gy of irradiation, and the mice were injected intraperitoneally with bromodeoxyuridine (BrdU) (1 mg) 1 h before sacrifice (48). Skin sections were treated with 3% hydrogen peroxidase for 15 min to quench endogenous peroxidase. BrdU was detected by using a BrdU staining kit (Oncogene Research Products) according to the manufacturer's protocol. For analysis of the $G_1$/S checkpoint in the thymus, 5- to 8-week-old mice were irradiated with 10 Gy of irradiation and injected with 2 mg of BrdU at 2 h postirradiation (3). At 1 h postinjection, the mice were sacrificed and the thymi were dissected. Thymocytes were fixed by using the BrdU flow kit (BD PharMingen). The fixed cells were treated with 300 μg of DNase/ml for 1 h at 37°C and then incubated with anti-BrdU-fluorescein isothiocyanate for 30 min at room temperature. After washing, the cells were counterstained with PI and subjected to flow cytometry. To detect mitotic cells, skin sections were incubated with anti-phosphohistone H3 antibody (Ab) (Upstate Biotechnology). After incubation with secondary Ab followed by Vectastain ABC reagents, the slides were exposed to DAB substrate (Vector Laboratories). Total cell numbers and the number of BrdU- or phosphohistone H3-positive cells were counted in several regions of the epidermis of each mouse.

$G_1$ arrest was examined in cultured mouse embryonic fibroblasts (MEFs) established as described previously (18). MEFs were synchronized at $G_0$ by incubation for 4 days in Dulbecco's minimal essential medium containing 0.1% serum. The $G_0$-synchronized cells were trypsinized and resuspended in growth medium containing 65 μM BrdU. The cells were irradiated with 0 to 20 Gy of irradiation, replated, and cultured for 24 h prior to fixation in 70% ethanol. Cells were then stained with anti-BrdU Ab (BD PharMingen) as described previously. To evaluate the S-phase checkpoint, the inhibition of DNA synthesis was measured by using a previously described procedure (27). Briefly, exponentially growing MEFs were irradiated with 10 Gy of irradiation and cultured for 0 to 3 h. [$^3$H]thymidine (2.5 μCi/ml) was added 30 min prior to sampling. Cells were lysed in 0.5 ml of 2% sodium dodecyl sulfate (SDS) in 0.2 M NaOH, and 100 μl of lysate was adsorbed onto Whatman 17 CHR paper. The filters were washed with 5% trichloroacetic acid, rinsed in 95% ethanol, and air dried, and the incorporated radioactivity was measured in a liquid scintillation counter.

**Northern blotting.** Thymocytes were subjected to 5 Gy of γ-irradiation, and total RNA was isolated by using Trizol according to the manufacturer's protocol (GIBCO BRL). Briefly, thymocytes ($2 \times 10^7$) were lysed with 1 ml of Trizol and mixed with chloroform. Total RNA was precipitated with isopropyl alcohol, and 5 μg/sample was electrophoresed on a 1% agarose gel followed by transfer to a membrane (GeneScreen plus; NEN Life Science Products). Blots were hybridized with mouse p21, Bax, and β-actin cDNA probes, and the intensity of each band was quantified by densitometry (Storm860; Molecular Dynamics). Statistical analyses were carried out by using Student's *t* test.

**Western blotting.** Tissues were lysed in lysis buffer (10 mM Tris-HCl [pH 7.5], 10 mM KCl, 2 mM $MgCl_2$, 1 mM dithiothreitol, 5 mM $Na_2P_2O_7$, 1 mM $Na_2VO_4$, and 50 mM NaF plus protease inhibitor cocktail [Boehringer Mannheim]). Lysates were boiled with SDS sample buffer at 100°C for 5 min and placed on ice. Protein extracts were fractionated by SDS–10% polyacrylamide gel electrophoresis and transferred to a polyvinylidene difluoride membrane (Sigma). The blot was incubated with 4% milk overnight followed by incubation with anti-p53 Ab (CM5; Novocastra Laboratories), anti-mouse Chk2 Ab (26), or anti-β-actin Ab (Sigma). Signals were visualized by incubation with horseradish peroxidase-conjugated secondary Ab (Amersham) followed by enhanced chemiluminescence (Amersham).

**Flow cytometric analysis.** The preparation of samples for flow cytometry was performed as described previously (26). Cells were analyzed on a Becton Dickinson FACScan.

**DMBA-induced skin tumor formation.** The backs of 6- to 8-week-old mice were shaved and painted with 10 μg of 7,12-dimethylbenzanthracene (DMBA) (Sigma) in 0.2 ml of acetone once a week for 25 weeks. Scoring for tumors was done once a week.

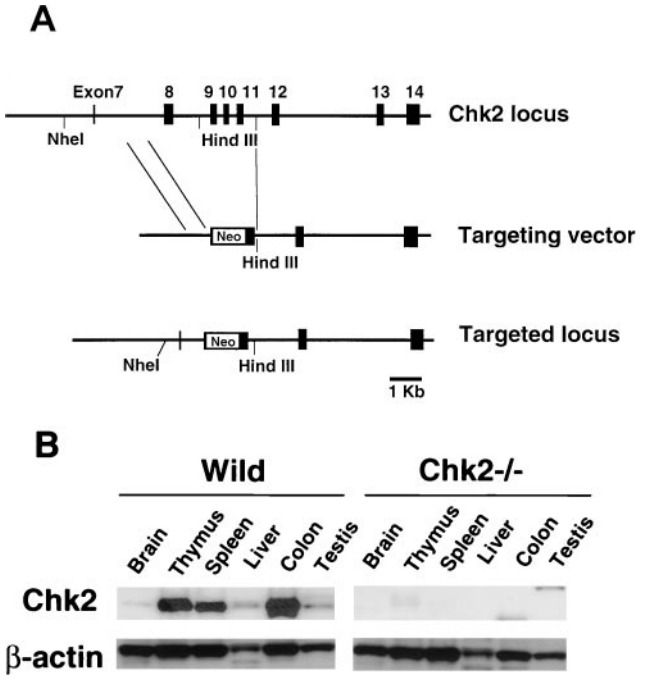


FIG. 1. Targeted disruption of the Chk2 gene in mice. (A) Targeting strategy. The genomic configuration of the germ line Chk2 locus is shown at the top. The targeting vector is shown in the center; exons 8 to 11 were replaced with a neomycin cassette (Neo). The mutated Chk2 locus is shown at the bottom. (B) Western blot showing the expression of Chk2 and β-actin proteins in various tissues of wild-type (Wild) and $Chk2^{-/-}$ mice.

**Reintroduction of Chk2 genes.** A *Bam*HI site was introduced into the 5′ end of the coding region of the mouse Chk2 cDNA by PCR. The full-length mouse Chk2 cDNA was cloned into pCAGGS (a gift of Junichi Miyazaki, Osaka University) with a blunt end. To create the mutated Chk2 allele, PCR-based mutagenesis was used to change the seven Ser-Gln/Thr-Gln (SQ/TQ) sites (Ser 22, 24, 29, 36, 42, and 59 and Thr77) in Chk2 to Ala-Gln (AQ) followed by subcloning into pCAGGS. To obtain thymocytes expressing wild-type or mutant Chk2, somatic chimeras were generated by $Rag1^{-/-}$ blastocyst complementation as previously described (26). pCAGGS-wild-type Chk2, pCAGGS-mutated Chk2,or the empty vector was electrophoretically transfected along with pBS-pgk-Hygro into $Chk2^{-/-}$ ES cells. At 48 h posttransfection, hygromycin (200 μg/μl) was added to the cultures. After 10 days, hygromycin-resistant clones were isolated and expanded. Clones with the highest expression of Chk2 were selected by Western blotting with anti-Chk2 Ab. Selected ES clones were injected into 3.5-day $Rag1^{-/-}$ blastocysts as described above to generate animals whose thymocytes had recovered Chk2 expression.

## RESULTS

**Generation of $Chk2^{-/-}$ mice.** The Chk2 gene was disrupted by replacing a region of the genomic sequence containing exons 8 to 11 with a neomycin resistance cassette (Fig. 1A). Following transfection, selection of targeted clones, and blastocyst microinjection, chimeric mice were produced that successfully transmitted the Chk2 mutation to the germ line. $F_1$ heterozygote mice were intercrossed to generate animals homozygous for the mutant Chk2 allele. $Chk2^{-/-}$ mice were viable and born at the expected Mendelian ratio (+/+:+/−:−/− = 0.20:0.53:0.26). The expression of Chk2 protein was assessed in $Chk2^{+/+}$ and $Chk2^{-/-}$ mice. The Chk2 protein is ubiquitously expressed in wild-type mouse tissues with its highest levels in the thymus, spleen, and colon (Fig. 1B). The protein was not detected in $Chk2^{-/-}$ tissues, confirming the null mutation.

**Chk2 is not essential for somatic growth, fertility, or immunological development.** Since Chk2 activation in response to DNA DSBs is dependent on ATM (34), we anticipated that $Chk2^{-/-}$ mice might display overlapping phenotypes with those of $ATM^{-/-}$ mice. We therefore investigated several of the most obvious phenotypes of $ATM^{-/-}$ mice in $Chk2^{-/-}$ animals.

$ATM^{-/-}$ mice are smaller in size and weigh less than their wild-type or heterozygous littermates (4, 21, 52). However, $Chk2^{-/-}$ mice were not smaller than control mice at birth, at weaning, or through adulthood (male, +/+ versus +/− versus −/−: 19.5 ± 3.4 g versus 23.1 ± 2.1 g versus 22.0 ± 2.6 g, respectively; female, +/+ versus +/− versus −/−: 18.2 ± 3.2 g versus 17.8 ± 1.3 g versus 17.9 ± 3.1 g, respectively) (42 days of age). In addition, while cultured MEFs from $ATM^{-/-}$ mice showed extremely poor growth consistent with the animals' growth retardation, cultured $Chk2^{-/-}$ fibroblasts did not show an obvious growth deficit (data not shown).

$ATM^{-/-}$ mice are infertile due to a defect in germ cell development. However, $Chk2^{-/-}$ male and female mice are fertile, and their gonads are histologically normal (data not shown).

Several immunological abnormalities have been reported in $ATM^{-/-}$ mice, including a defect in T-lymphocyte maturation. However, lymphoid tissues from $Chk2^{-/-}$ mice were similar in gross size to those of their $Chk2^{+/-}$ and wild-type littermates, and no histological abnormalities were observed in the thymus, spleen, or lymph nodes. The numbers of thymocytes and spleen cells isolated from $Chk2^{-/-}$ mice were comparable to those of the controls at 8 to 10 weeks of age. Analysis of cell surface markers of isolated $Chk2^{-/-}$ lymphoid cells showed that populations of cells bearing CD3, CD4, CD8, Thy1, or T-cell receptor αβ were not affected by the loss of Chk2 in either the thymus or the spleen. The development of immature T cells, as evaluated by CD25 and CD44 expression, was also normal. Analysis of the expression of B220, immunoglobulin D (IgD), IgM, and CD43 in spleen and bone marrow cells revealed no abnormalities in B-cell development. The proliferation of peripheral lymph node T cells stimulated with anti-CD3 Ab, anti-CD28 Ab, and interleukin-2 was normal, as was that of splenic B cells stimulated with anti-CD40 Ab, anti-IgM Ab, interleukin-4, or lipopolysaccharide. Immunoglobulin levels in $Chk2^{-/-}$ mice were normal.

**Apoptosis and cell cycle arrest induced by IR are defective in $Chk2^{-/-}$ mice.** In our previous work, we showed that $CD4^+$ $CD8^+$ thymocytes isolated from $Chk2^{-/-}$ $Rag1^{-/-}$ chimeric animals were resistant to IR-induced apoptosis because of a lack of p53 stabilization. In this study, we evaluated the role of Chk2 in regulating IR-induced cell death in vivo. Wild-type and $Chk2^{-/-}$ mice were subjected to whole-body γ-irradiation, and their thymic tissues were evaluated for apoptosis by using the TUNEL assay. Thymi of unirradiated wild-type and $Chk2^{-/-}$ mice showed very few apoptotic cells (Fig. 2A). As expected, substantial apoptosis was observed in the thymi of irradiated wild-type mice. However, the thymi of irradiated $Chk2^{-/-}$ mice showed significantly less apoptosis. We next examined the effect of the Chk2 mutation on hair follicular

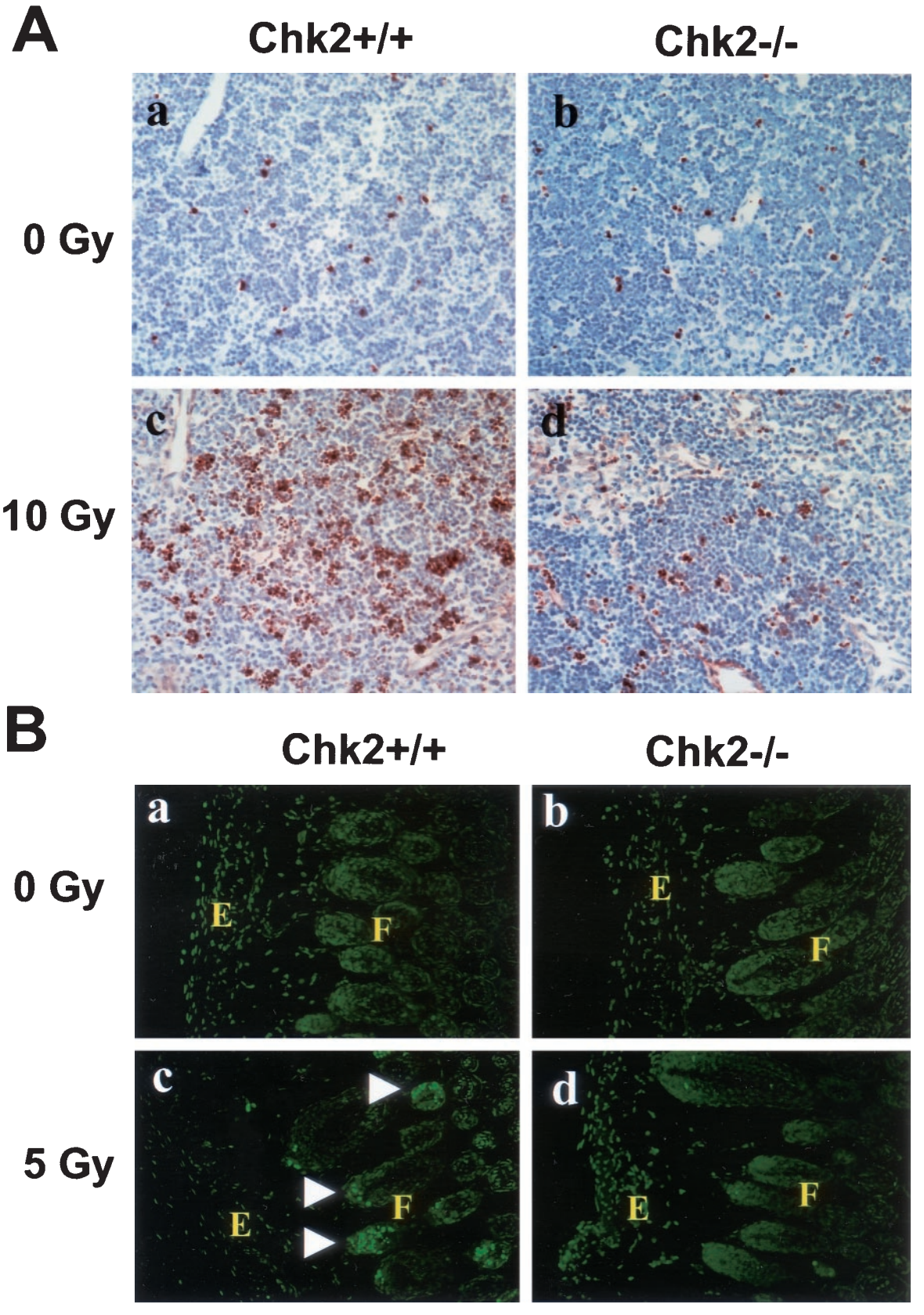


FIG. 2. Induction of apoptosis in response to γ-irradiation. (A) Mice (8 weeks old) were mock irradiated (a and b) or irradiated with 10 Gy of irradiation (c and d), and apoptosis in thymi was evaluated at 10 h post-IR. (B) Mice (P7) were mock irradiated (a and b) or irradiated with 5 Gy of irradiation (c and d), and apoptosis in skin was evaluated at 6 h post-IR by in situ TUNEL staining. E and F indicate epidermis and hair follicle, respectively. (C) Mice (P5) were mock irradiated (a and b) or irradiated with 10 Gy of irradiation (c and d), and apoptosis in the hippocampal dentate gyrus was evaluated at 24 h post-IR by in situ TUNEL staining. Arrows indicate apoptotic TUNEL-positive cells.

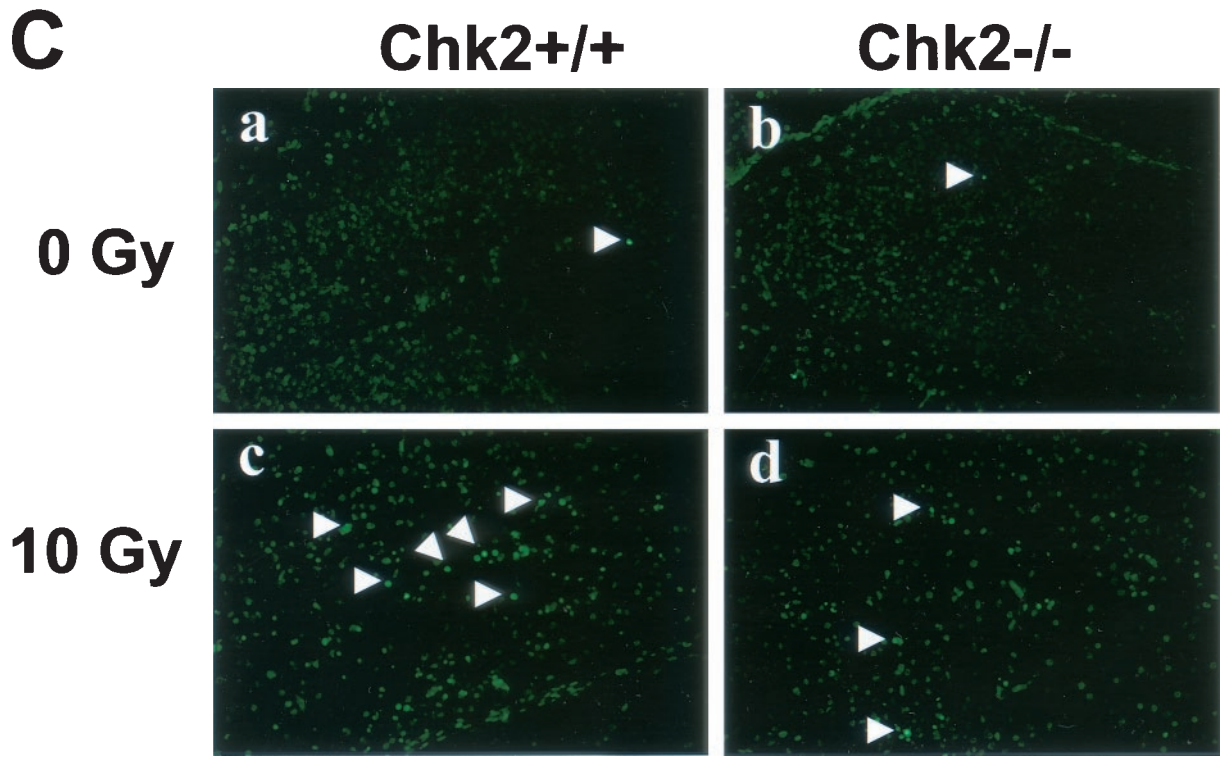


FIG. 2—*Continued.*

matrical cells since these cells have been shown to be susceptible to IR-induced apoptosis (4, 48). Four hours after 5 Gy of irradiation, a large number of cells in the wild-type matrix were undergoing apoptosis, as evaluated by an in situ TUNEL assay (Fig. 2B). In contrast, there was an almost complete absence of IR-induced apoptosis in the follicular matrices of $Chk2^{-/-}$ mice. Finally, we examined IR-induced apoptosis in the developing CNS. In wild-type perinatal mice (P5), significant apoptosis was observed in many regions of the CNS 24 h after 5 Gy of γ-irradiation, consistent with previous reports. Strikingly, very little apoptosis was observed in the CNS, including the cerebellum and dentate gyrus, of irradiated $Chk2^{-/-}$ mice (Fig. 2C and data not shown).

Since IR induces cell cycle arrest at several distinct cell cycle transitions, we studied the effect of the absence of Chk2 on the $G_1$/S, S, and $G_2$/M checkpoints. First, we examined the $G_1$/S checkpoint in epidermal cells in vivo. P7 mice were irradiated with 5 Gy of irradiation followed by BrdU injection 1 h prior to sacrifice. The frequency of BrdU-positive cells in $Chk2^{-/-}$ epidermis was comparable to that in wild-type tissue (wild type versus $Chk2^{-/-}$: 108 ± 13 per 1,000 cells versus 110 ± 15 per 1,000 cells). Although epidermal cells are not susceptible to IR-induced apoptosis, there was a clear reduction in the BrdU-positive population in the wild type at 24 h postirradiation (21 ± 5 per 1,000 epidermal cells), likely due to the operation of the $G_1$/S checkpoint (Fig. 3A). In contrast, there was no reduction in the BrdU-positive population at 24 h in either $Chk2^{-/-}$ epidermis (112 ± 10 per 1,000 cells) or in $p53^{-/-}$ epidermis (132 ± 7 per 1,000 cells). $G_1$ arrest was also evaluated in cultured wild-type, $p53^{-/-}$, and $Chk2^{-/-}$ MEFs. Serum-starved cells were irradiated and stimulated to enter the cell cycle by the addition of serum. BrdU was added with the serum to allow the detection of S-phase entrance. In response to increasing doses of IR, $p53^{-/-}$ MEFs failed to arrest in $G_1$, as expected (Fig. 3B) (18). Wild-type MEFs arrested normally in $G_1$ as evidenced by a dose-dependent reduction in the number of BrdU-positive cells. Interestingly, $Chk2^{-/-}$ MEFs were significantly defective in their ability to arrest in $G_1$ at low IR doses but behaved like wild-type cells at higher doses.

To examine the $G_2$/M checkpoint, we used an anti-phosphohistone H3 Ab which specifically recognizes mitotic cells to evaluate the frequency of mitotic cells in the epidermis following IR. In the absence of IR, the frequency of mitotic cells was comparable in wild-type and $Chk2^{-/-}$ mice (wild type versus $Chk2^{-/-}$: 18 ± 4 per 1,000 cells versus 20 ± 4 per 1,000 cells) (Fig. 3C). Almost no mitotic cells were observed in wild-type or $Chk2^{-/-}$ mice 6 h after exposure to 5 Gy of irradiation, indicating that the induction of $G_2$ arrest is intact in $Chk2^{-/-}$ mice. However, mitosis had resumed in $Chk2^{-/-}$ cells by 24 h post-IR (21 ± 4 per 1,000 cells), whereas wild-type cells still showed suppression of mitosis (3 ± 2 per 1,000 cells) at this time. These data indicate that the loss of Chk2 curtails the duration of the $G_2$/M checkpoint.

An intra-S-phase checkpoint occurs in MEFs in response to IR, and this checkpoint requires ATM function (4). We evaluated the effect of the Chk2 mutation on this checkpoint by examining the inhibition of DNA synthesis in MEFs. Both wild-type and $Chk2^{-/-}$ primary MEFs showed equivalent levels of DNA synthesis inhibition following IR, whereas $ATM^{-/-}$ cells showed a characteristic profile of radiation-

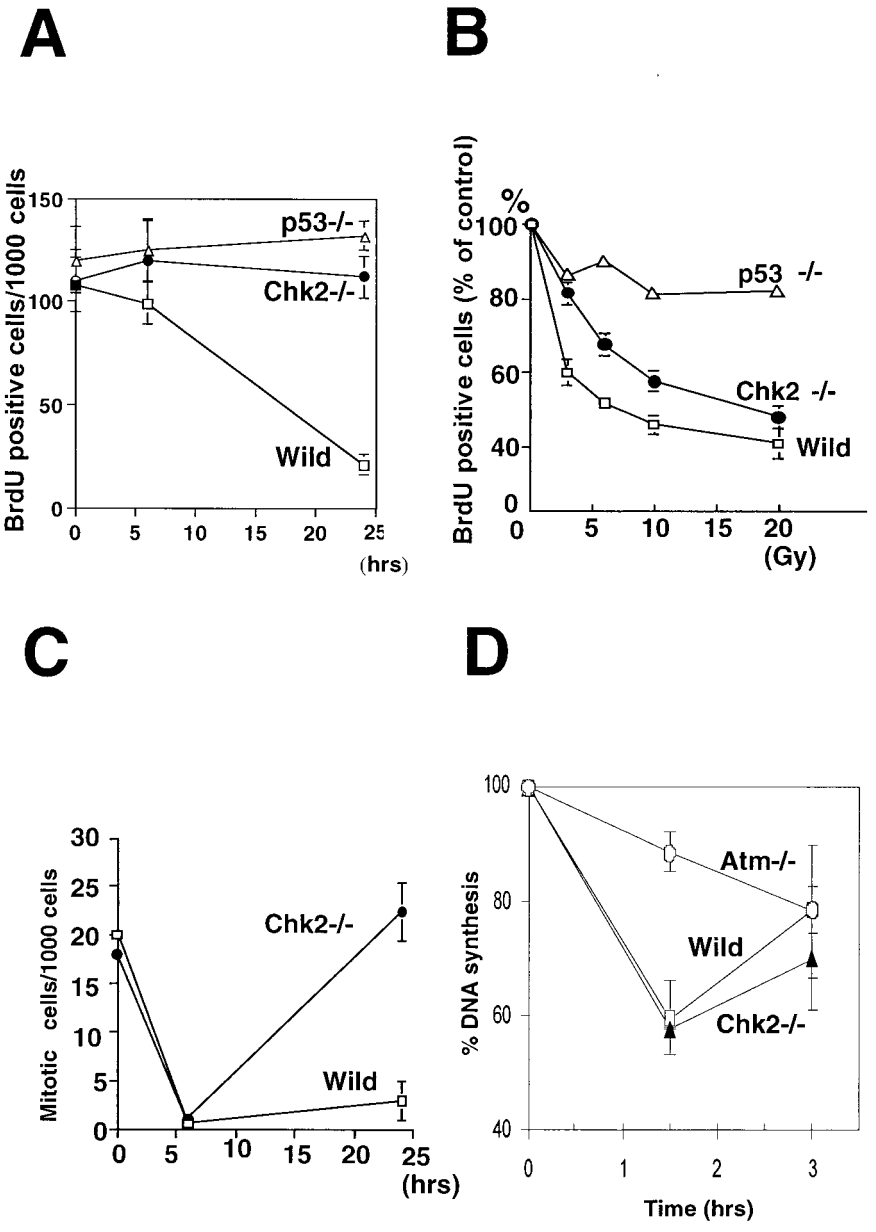


FIG. 3. Cell cycle checkpoints induced by γ-irradiation of wild-type (wild) and Chk2$^{-/-}$ mice. (A) $G_1$/S checkpoint in the epidermis. Mice (P7) were irradiated with 5 Gy of irradiation, and BrdU was injected 1 h prior to sacrifice. BrdU-positive cells were taken as those in S phase. Each value represents the mean number ± standard deviation (SD) of BrdU-positive cells from 3 mice per group. (B) $G_1$/S checkpoint in MEFs. MEFs were synchronized in $G_0$ by serum starvation and irradiated with 0 to 20 Gy of irradiation as indicated. The irradiated cells were incubated with BrdU, and S-phase cells were detected by flow cytometric analysis of anti-BrdU Ab binding. Each value represents the mean percentage ± SD of BrdU-positive cells present after IR in 5 cultures per group relative to the unirradiated controls. (C) $G_2$/M checkpoint in epidermis. Mice (P7) were irradiated with 5 Gy of irradiation, and mitotic cells in the epidermis were detected with anti-phosphohistone H3 Ab. Each value represents the mean number ± SD of mitotic cells from 3 mice per group. (D) S-phase checkpoint in primary MEFs. Exponentially growing primary MEFs were irradiated with 10 Gy of irradiation and sampled at the post-IR times indicated. [$^3$H]thymidine was added for 30 min prior to sampling, and [$^3$H]thymidine incorporation was determined in the cell lysates. The results are expressed as percentages of DNA synthesis relative to label incorporated in unirradiated cells. Each point represents the mean ± SD of 3 to 5 samples per group.

resistant DNA synthesis (Fig. 3D). These findings show that the intra-S-phase checkpoint is ATM dependent but Chk2 independent.

**Incidence of DMBA-induced skin tumors is enhanced in Chk2-deficient mice.** Since the loss of Chk2 leads to suppressed apoptosis and cell cycle arrest in response to IR, one would expect to find a higher incidence of tumor formation in Chk2$^{-/-}$ mice, perhaps comparable to that in p53$^{-/-}$ mice. However, by age 1 year, Chk2$^{-/-}$ mice had not developed tumors of any kind. We speculate that tumors caused by the loss of Chk2 are either too rare to be detected or require a prolonged period to develop. We therefore challenged

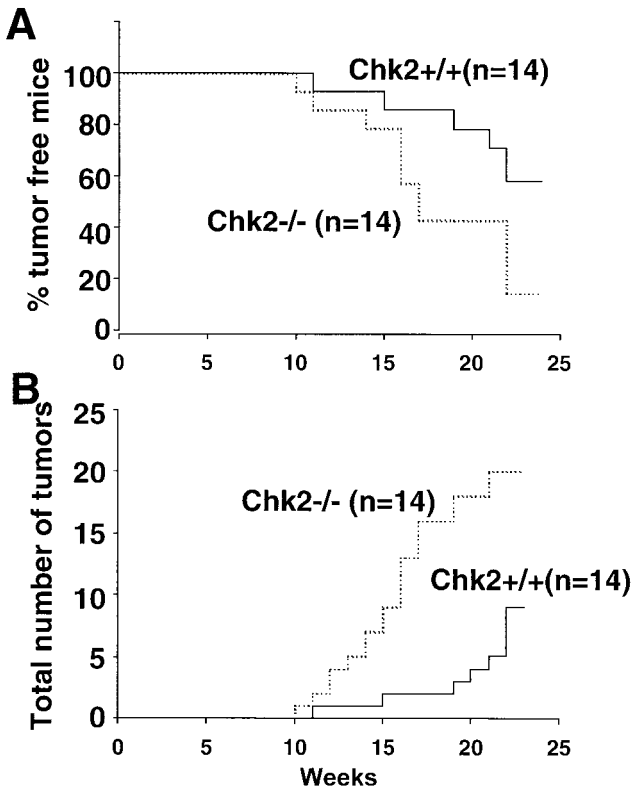


FIG. 4. Skin tumor formation in mice treated with DMBA. The back skin of 6- to 8-week-old mice was shaved and painted with 10 μg of DMBA once a week for 25 weeks. Tumors in skin were scored once a week. (A) Kaplan-Meier plot of tumor incidence in wild-type ($n$ = 14) and Chk2$^{-/-}$ ($n$ = 14) mice. (B) Total numbers of tumors in mice for which data are shown in panel A.

Chk2$^{-/-}$ mice with the chemical carcinogen DMBA, an agent that damages DNA and efficiently induces skin tumors (15, 40). More Chk2$^{-/-}$ mice than wild-type animals developed skin tumors in response to DMBA treatment (wild type versus Chk2$^{-/-}$: 6 of 14 versus 12 of 14 at 25 weeks) (Fig. 4A). The onset of tumors in Chk2$^{-/-}$ mice occurred earlier than in wild-type animals, and the total number of tumors was increased in Chk2$^{-/-}$ mice compared to wild-type mice (Fig. 4B). However, the size of individual tumors and the frequency of malignant tumors (carcinomas) were comparable between wild-type and Chk2$^{-/-}$ mice. We conclude that Chk2 has a suppressive effect on tumor development induced by at least some types of DNA damage.

**Chk2 selectively regulates apoptosis in an ATM-independent manner.** Although Chk2 acts downstream of ATM in yeast and mammals, the loss of Chk2 does not result in many of the phenotypes observed in ATM$^{-/-}$ mice. In fact, the only shared phenotype is defective p53 function in response to IR. This finding prompted us to explore the possibility that Chk2 and ATM might have different regulatory effects on p53 function. Whereas Chk2$^{-/-}$ cells have a clear defect in IR-induced apoptosis, this phenotype is variable in ATM$^{-/-}$ cells. We therefore carefully compared the effect of the loss of Chk2 or ATM on the regulation of p53 activation in thymocytes. p53-mediated cell cycle arrest and apoptosis have been well characterized in thymocytes, and it is possible to precisely quantify these phenotypes in this cell type. When wild-type mice were subjected to 10 Gy of γ-irradiation, the number of thymic BrdU-positive S-phase cells was reduced to 35% ± 4% of that in the nonirradiated controls (Fig. 5A). The $G_1$/S-phase checkpoint was defective in ATM$^{-/-}$ and p53$^{-/-}$ mice (ATM$^{-/-}$, 132% ± 10%; p53$^{-/-}$, 128% ± 11%), consistent with previous reports (3). In contrast to irradiated ATM$^{-/-}$ mice, irradiated Chk2$^{-/-}$ mice showed only a partial defect that resulted in milder $G_1$ arrest (65% ± 5%). However, when thymocytes were isolated from Chk2$^{-/-}$ mice and subjected to IR in vitro, apoptosis was dramatically impaired (Fig. 5B). ATM$^{-/-}$ thymocytes were more resistant than wild-type thymocytes to IR-induced apoptosis but considerably more sensitive than either Chk2$^{-/-}$ or p53$^{-/-}$ thymocytes. It should be noted that the IR-induced apoptosis and inhibition of the $G_1$/S transition observed in this study are p53 dependent because they are completely inhibited by the loss of p53 function. Dying p53$^{-/-}$ thymocytes can be detected after 48 h of IR treatment, and irradiated Chk2$^{-/-}$ p53$^{-/-}$ thymocytes behave in the same manner as irradiated p53$^{-/-}$ cells (data not shown). These results indicate that Chk2 acts in the pathway leading to p53-dependent apoptosis rather than in the general apoptosis program.

Our findings led us to hypothesize that Chk2 selectively regulates p53 activity leading to apoptosis. To address this question, we used Northern blotting to evaluate the transactivation of mRNA expression for known p53 target genes. Although the expression of many molecules is induced by p53 activation, p21 and Bax are the most prominent p53-responsive genes in mouse primary thymocytes (8). Loss of p21 in thymocytes leads to a clear defect of the $G_1$ checkpoint induced by IR (18). Although Bax$^{-/-}$ thymocytes are not resistant to IR-induced apoptosis, Bax$^{-/-}$ Bak$^{-/-}$ thymocytes fail to die in response to IR (32). Since Bak$^{-/-}$ thymocytes also show normal responses to IR, the induction of Bax must be critical for IR-induced apoptosis. In wild-type thymocytes subjected to 5 Gy of IR, Bax mRNA was increased by (6.05 ± 1.44)-fold over the baseline at 3 h and by (5.68 ± 1.64)-fold at 6 h (Fig. 5C, left panel). Strikingly, irradiated Chk2$^{-/-}$ thymocytes showed defective induction of Bax ([1.9 ± 0.45]-fold at 3 h and [1.80 ± 0.40]-fold at 6 h). These results represent statistically significant decreases compared to the wild type at 3 h ($P < 0.01$) and 6 h ($P < 0.01$). In contrast, irradiated ATM$^{-/-}$ thymocytes were slower than the wild-type to induce Bax mRNA synthesis at 3 h ($P < 0.05$) but had caught up by 6 h. p21 mRNA induction was significantly suppressed compared to that of the wild type ($P < 0.05$) in both ATM$^{-/-}$ and Chk2$^{-/-}$ irradiated thymocytes at 3 h (Fig. 5C, right panel), but there were no significant differences in the level of suppression between these two genotypes. Consistent with a previous report (3), neither p21 nor Bax was induced in irradiated p53$^{-/-}$ thymocytes. These results suggest that thymic apoptosis induced by IR depends on p53 function and is controlled mainly by Chk2 rather than ATM. p53 was stabilized partially by IR in both ATM$^{-/-}$ and Chk2$^{-/-}$ thymocytes (Fig. 5D). Taken together, the data in Fig. 5 demonstrate that Chk2, rather than ATM, controls p53-mediated apoptosis, and that p53-mediated apoptosis does not correlate with stabilization of the p53 protein.

We next determined whether Chk2 phosphorylation is re-

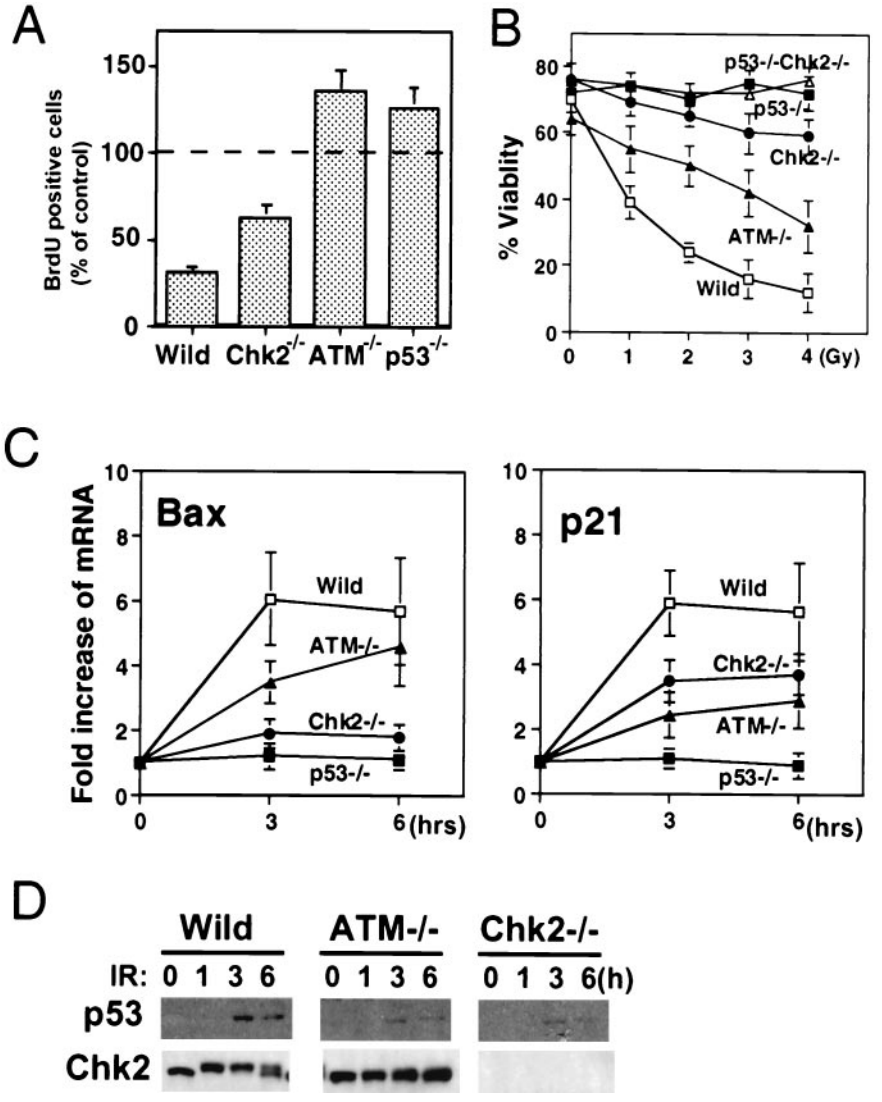


FIG. 5. IR-induced p53 activation and p53 stabilization in Chk2$^{-/-}$ and ATM$^{-/-}$ thymocytes. (A) $G_1$/S checkpoint induced by γ-irradiation. The indicated strains of mice were irradiated with 10 Gy of irradiation and injected 1 h later with BrdU. At 2 h post-IR, thymocytes were isolated, stained with anti-BrdU Ab, and subjected to flow cytometry. Each value represents the mean percentage ± standard deviation (SD) of BrdU-positive (S phase) cells present after IR in 4 samples per group relative to the unirradiated controls. (B) Apoptosis induced by γ-irradiation. Isolated thymocytes were treated with the indicated doses of γ-irradiation, and apoptotic cells were evaluated by flow cytometry after Annexin V and PI staining. Each value represents the mean percentage ± SD of viable cells (Annexin V negative and PI negative) for 4 samples per group. (C) Induction of p53 downstream molecules. Total RNA was isolated from thymocytes before and after treatment with 5 Gy of irradiation. The expression of mRNA for p21, Bax, and β-actin was evaluated by Northern blotting. The amount of p21 or Bax mRNA was quantified by using a PhosphorImager analyzer and normalized to β-actin expression. Each value represents the mean increase (*n*-fold) ± SD of the expression of Bax or p21 mRNA after IR in 3 to 5 samples per group relative to the unirradiated controls. (D) p53 protein stabilization and Chk2 phosphorylation in thymocytes after irradiation. Isolated thymocytes were irradiated with 5 Gy of irradiation and lysed at the indicated times. p53 and Chk2 proteins were detected by Western blotting with anti-p53 or anti-Chk2 Ab. Wild, wild type.

quired for the activation of p53 leading to apoptosis. Mouse Chk2 has seven N-terminal SQ/TQ sites in the N-terminal region of the protein. In response to IR in vivo, ATM phosphorylates several of these SQ/TQ sites in Chk2, including Thr68 (1, 35, 36). Phosphorylation of Chk2 following IR is abolished by mutation of these SQ/TQ sites, and most of the endogenous Chk2 is not phosphorylated in ATM$^{-/-}$ cells (Fig. 5D); nevertheless, p53-mediated apoptosis can occur under these circumstances. To determine whether the phosphorylation of Chk2 SQ/TQ sites is required for Chk2-mediated regulation of p53-mediated apoptosis, we reintroduced into Chk2$^{-/-}$ thymocytes a mutant form of Chk2 in which all N-terminal SQ/TQ sites were replaced with AQ and analyzed apoptosis. In a previous study (35), the mutated SQ/TQ kinase had the same level of kinase activity as the wild-type enzyme when transfected into unirradiated Chk2$^{-/-}$ MEFs. To reintroduce the mutated Chk2 gene into Chk2$^{-/-}$ thymocytes, we generated somatic chimeras by Rag1$^{-/-}$ blastocyst complementation. An expression vector carrying wild-type or mutant Chk2 was transfected into Chk2$^{-/-}$ ES cells, and clones with

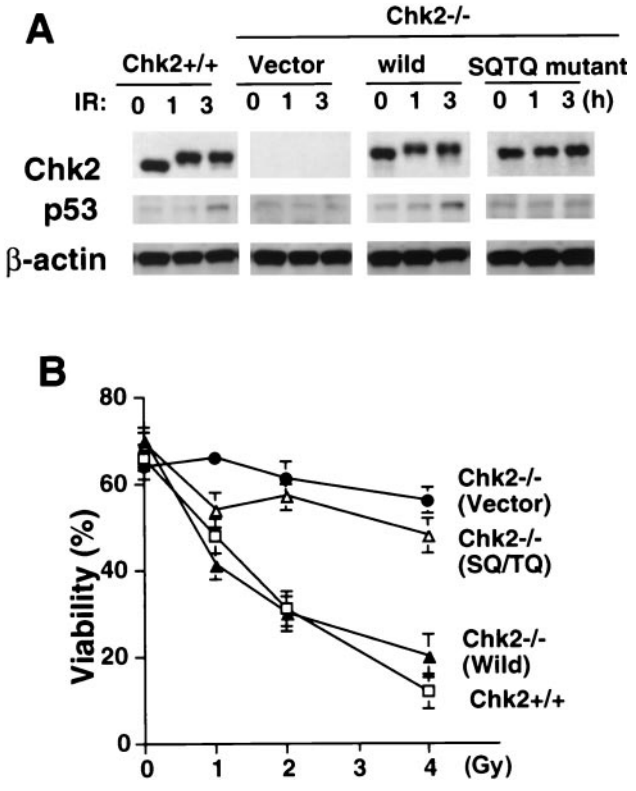


FIG. 6. Effect of reintroduced mutant Chk2 on IR-induced apoptosis. $Chk2^{-/-}$ ES cells transfected with either empty vector (vector), vector containing wild-type Chk2 (wild), or vector containing the Chk2 SQ/TQ mutant gene (SQ/TQ mutant) were injected into blastocysts from $Rag1^{-/-}$ mice to generate chimeric animals expressing the corresponding proteins in thymocytes. (A) Expression of reintroduced Chk2 protein and stabilization of p53 following 5 Gy of γ-irradiation for the indicated times. (B) Thymocytes isolated from the chimeric mice for which data are shown in panel A were irradiated at the indicated doses. Apoptosis was analyzed by Annexin V-PI staining at 24 h post-IR. Each value represents the mean percentage ± standard deviation of viable cells in 3 cultures per group.

high expression of Chk2 protein were selected and used for blastocyst complementation. The size and cellularity of thymi in $Chk2^{-/-}$ mice bearing an empty vector, $Chk2^{-/-}$ mice bearing wild-type Chk2, and $Chk2^{-/-}$ mice bearing the mutated Chk2 were all comparable to those of control wild-type mice (data not shown). Moreover, the expression level of the exogenous Chk2 protein was comparable to that of the endogenous Chk2 protein. Exogenous wild-type Chk2 was phosphorylated in response to IR, whereas the mutated Chk2 protein failed to show a mobility shift (Fig. 6A). Thus, the defective p53 stabilization in $Chk2^{-/-}$ thymocytes was restored by the introduction of exogenous wild-type Chk2 but not by mutant Chk2. Reintroduction of wild-type Chk2 also clearly restored the defective apoptosis observed in $Chk2^{-/-}$ thymocytes (Fig. 6B), whereas thymocytes receiving mutant Chk2 behaved similarly to control $Chk2^{-/-}$ thymocytes. These data suggest that phosphorylation of the SQ/TQ sites in Chk2 is required for this protein to induce ATM-independent p53 activation leading to apoptosis.

## DISCUSSION

We have shown in this study that there are differences between $Chk2^{-/-}$ and $ATM^{-/-}$ cells in the IR-induced activation of checkpoint and apoptotic responses, despite the fact that ATM regulates IR-induced Chk2 activity. ATM and Chk2 both modify p53 and activate it; however, our results show that at least some p53 phosphorylation is Chk2 dependent and ATM independent. Moreover, Chk2-dependent and ATM-dependent p53 phosphorylation events may differentially affect downstream p53-dependent transactivation targets. Specifically, we have demonstrated that Chk2 predominantly regulates IR-induced apoptosis rather than the $G_1$/S checkpoint in thymocytes, whereas ATM is predominantly involved in the regulation of the $G_1$/S checkpoint.

Contradictory results have been reported regarding the effect of ATM on p53-mediated apoptosis (3, 21, 24, 53). The discrepancies among these reports are not caused by strain differences among experimental mice but could be due to differences in methods used to detect apoptosis or to irradiation conditions (in vivo versus ex vivo). The in situ TUNEL assay may not be sensitive enough to detect differences in apoptosis in a thymus taken from an $ATM^{-/-}$ mouse treated with whole-body irradiation, whereas in vitro irradiation of isolated $ATM^{-/-}$ thymocytes reveals an apoptotic defect. In contrast, $Chk2^{-/-}$ thymocytes examined using either method show obvious resistance to IR-induced apoptosis. In our study, $ATM^{-/-}$ thymocytes were more resistant than the wild type to IR but significantly less resistant than $Chk2^{-/-}$ thymocytes. Consistent with the results of the apoptosis assay, the induction of Bax mRNA was more profoundly impaired in $Chk2^{-/-}$ thymocytes than in $ATM^{-/-}$ cells. This tight correlation between the induction of apoptosis and the transactivation of p53 downstream molecules suggests that the inhibition of apoptosis induced by the loss of Chk2 is caused by the suppression of p53 activation itself and not by effects on molecules further downstream in the apoptosis pathway.

We and others have proposed a model of IR-induced p53 activation in which Chk2 phosphorylates Ser20 of p53, leading to stabilization of p53 protein in an ATM-dependent manner (11, 26). Certainly, p53 stabilization was suppressed in both $Chk2^{-/-}$ and $ATM^{-/-}$ mice. However, the loss of ATM or Chk2 had different effects on p53 activation leading to apoptosis, indicating that the regulation of IR-induced p53 activation is not as simple as proposed above. Both ATM and Chk2 are required for p53 stabilization, but Chk2 must have another effect on p53 function in addition to stabilization that promotes apoptosis in response to IR (Fig. 7). Loss of Chk2 does lead to a defect of the $G_1$/S checkpoint, but this could be caused by defective p53 protein stabilization. A similar explanation could hold for the partial effect of the ATM mutation on apoptosis.

The mechanism underlying the regulation of p53 activation remains unknown, but a key candidate is phosphorylation since p53 is phosphorylated on many sites in response to DNA damage. Regulation of p53 activation by Chk2 could involve the phosphorylation of additional sites on p53 or of other molecules that affect p53 activation. For example, the phosphorylation of Ser46 on p53 is specifically required for the induction of p53AIP1, a gene inducing apoptotic cell death. Mutation of Ser46 abolishes the ability of p53 to induce apo-

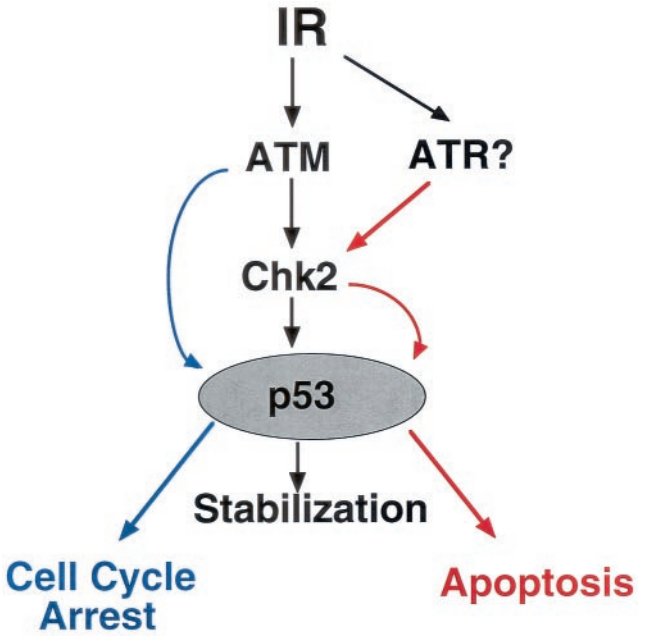


FIG. 7. Model of the regulation of p53 activation by Chk2 in response to IR. Chk2-mediated stabilization of p53 induced by IR and leading to apoptosis is controlled independently of ATM, possibly by ATR. ATM appears to stabilize p53, leading to cell cycle arrest without involving Chk2.

ptosis and selectively blocks transcription of p53AIP (but not other p53 target genes) (38). These data suggest that posttranslational modification of the p53 protein may determine its affinity for specific p53 binding sequences present in different target genes. Unfortunately, we do not know if Chk2 affects phosphorylation of Ser46 and p53AIP1 because Ser46 on human p53 is not conserved in mouse p53. It remains possible that other types of p53 modifications such as acetylation could lead to apoptosis via Chk2.

Mutation of the SQ/TQ sites on Chk2 abolished p53 activation leading to apoptosis, demonstrating that the phosphorylation of the SQ/TQ sites in the N-terminal region of Chk2 is essential for this process. Most of the phosphorylation of Chk2 induced by IR is abolished if ATM is absent. However, our data suggest that there is some ATM-independent phosphorylation at SQ/TQ sites of Chk2 in response to IR. It is possible that the very low level of ATM-independent phosphorylation of Chk2 that occurs is insufficient to alter the mobility of the protein. The most likely agent of ATM-independent Chk2 phosphorylation is ATR, although other members of the phosphatidylinositol 3-kinase family are also possibilities. ATR is a phosphatidylinositol 3-kinase-related kinase which contains a protein kinase domain similar in sequence to a region of *Schizosaccharomyces pombe rad3* (6, 13). Matsuoka et al. have reported that ATR phosphorylates Thr26, Ser50, and Thr68 in the SQ/TQ cluster domain of human Chk2 in vitro (35). Although ATR is believed to act primarily in response to a DNA replication block or UV-irradiation, it is also involved in responses to IR. Cells lacking ATR die within several days of exposure to IR; however, prior to their deaths, a profound defect in the IR-induced $G_2$/M checkpoint can be demonstrated (16). Other studies have shown that overexpression of a kinase-dead mutation of ATR causes increased sensitivity to IR and a defect in the $G_2$/M arrest and S-phase checkpoints (14). Furthermore, ATR mutation also abolishes DNA damage-induced phosphorylation of Ser15 on p53 (49). These data suggest a potential functional overlap between ATM and ATR with respect to IR responses, consistent with our hypothesis that ATM and ATR cooperate in regulating p53 activity (Fig. 7). We theorize that ATR selectively regulates p53 activation leading to apoptosis via Chk2, while ATM governs cell cycle arrest in a Chk2-independent manner.

In addition to phosphorylating p53, Chk2 is known to phosphorylate Cdc25. It has been reported that ATM and Chk2 are required for the S-phase checkpoint induced by IR and that this induction depends on Chk2-dependent phosphorylation of Cdc25A (22). In our study, we confirm that ATM is required for the S-phase checkpoint in primary MEFs but we also demonstrate that Chk2 is dispensable for this checkpoint in this cell type. In experiments with immortalized MEFs, we have observed a slightly slower onset and shorter duration of the S-phase checkpoint in the absence of Chk2 (unpublished data). This small difference may reflect differences in cell cycle parameters between primary and transformed cells. On balance, however, we believe that Chk2 is not essential for S-phase arrest in normal cells. It is possible that Chk1 can substitute for Chk2 in the phosphorylation of Cdc25 and that Chk2 thus has a redundant function in the intra-S-phase checkpoint. Previous reports concluding that Chk2 was required for the intra-S-phase checkpoint utilized overexpression constructs containing mutated Chk2 genes identified in sporadic colon cancer and as a germ line mutation in Li-Fraumeni syndrome (LFS). The data showed that these mutations had a dominant-negative impact in wild-type cells. Constructs containing such mutations could therefore have an inhibitory effect on a downstream component of the S-phase checkpoint (such as Cdc25), thereby preventing the operation of any compensatory Chk1-dependent process. Alternatively, differences in Chk2 dependency in different tissues or between mice and humans may underlie the discrepancy between the previous reports and our data.

Failures in the transcriptional response to damage, cell cycle arrest and apoptosis induced by IR should lead to a higher incidence of tumor development. Unexpectedly, however, $Chk2^{-/-}$ mice do not have obvious tumors, unlike $ATM^{-/-}$ mice, which die within 4 months of birth with thymic lymphomas. Interestingly, the thymic lymphomas in $ATM^{-/-}$ mice are critically dependent on V(D)J recombination, whereas thymic lymphomas in $p53^{-/-}$ mice arise independent of V(D)J recombination (30). These observations indicate that at least two different mechanisms of lymphoma development are at work in these mutant animals, such that ATM-mediated p53 activation may not be required for the development of lymphomas. ATM phosphorylates many target substrates in addition to Chk2 and p53, including Nbs1 and Brca1 (17, 31). These molecules, which act downstream of ATM, may contribute in an unknown way to the prevention of spontaneous lymphoma development.

Mutations of Chk2 are found more frequently in patients with variant LFS, which has a moderate phenotype, than in patients with classical LFS (5). In contrast, mutations of p53 have been reported in 70% of classical LFS cases and 20% of variant LFS patients (50). Although the tumor-suppressive ef-

fect of Chk2 appears to be milder than that of p53, loss of Chk2 clearly increased the incidence of DMBA-induced skin tumors in mice. DBMA treatment resembles UV-irradiation in that both cause DNA adducts that are repaired by the nucleotide excision repair system. This similarity in DNA lesions suggests that the DBMA-induced skin tumors appearing in $Chk2^{-/-}$ mice could be the result of a failure in the tumor-suppressive effect by ATR.

In conclusion, the results of this study have shown that p53 activation leading to cell cycle arrest is regulated differently from that leading to apoptosis. Chk2 is required for p53-mediated apoptosis of thymocytes and must undergo phosphorylation in order to function, but this phosphorylation is not carried out by ATM. We propose a new model for the IR pathway that emphasizes the independent effects of Chk2 and ATM.

## ACKNOWLEDGMENTS

We thank Malte Peters, Atsushi Togawa, and Katsuya Tsuchihara for helpful discussions, Peter J. McKinnon for providing $ATM^{-/-}$ mice, Junichi Miyazaki for providing pCAGGS, Mary Saunders for scientific editing, Denis Bouchard for technical expertise, and Irene Ng for excellent administrative support.

T.W.M. was supported by grants from the Canadian Institutes of Health Research (CIHR) and the National Cancer Institute of Canada (NCI). S.J.E. was supported by a DAMD grant. P.A.J. was supported by the industry-funded UKCCCR Radiation Research Programme, the Leukemia Research Fund, and European Union grant Figh CT 1999.

## REFERENCES

1. **Ahn, J. Y., J. K. Schwarz, H. Piwnica-Worms, and C. E. Canman.** 2000. Threonine 68 phosphorylation by ataxia telangiectasia mutated is required for efficient activation of Chk2 in response to ionizing radiation. Cancer Res. **60:**5934–5936.
2. **Banin, S., L. Moyal, S. Shieh, Y. Taya, C. W. Anderson, L. Chessa, N. I. Smorodinsky, C. Prives, Y. Reiss, Y. Shiloh, and Y. Ziv.** 1998. Enhanced phosphorylation of p53 by ATM in response to DNA damage. Science **281:**1674–1677.
3. **Barlow, C., K. D. Brown, C. X. Deng, D. A. Tagle, and A. Wynshaw-Boris.** 1997. Atm selectively regulates distinct p53-dependent cell-cycle checkpoint and apoptotic pathways. Nat. Genet. **17:**453–456.
4. **Barlow, C., S. Hirotsune, R. Paylor, M. Liyanage, M. Eckhaus, F. Collins, Y. Shiloh, J. N. Crawley, T. Ried, D. Tagle, and A. Wynshaw-Boris.** 1996. Atm-deficient mice: a paradigm of ataxia telangiectasia. Cell **86:**159–171.
5. **Bell, D. W., J. M. Varley, T. E. Szydlo, D. H. Kang, D. C. Wahrer, K. E. Shannon, M. Lubratovich, S. J. Verselis, K. J. Isselbacher, J. F. Fraumeni, J. M. Birch, F. P. Li, J. E. Garber, and D. A. Haber.** 1999. Heterozygous germ line hCHK2 mutations in Li-Fraumeni syndrome. Science **286:**2528–2531.
6. **Bentley, N. J., D. A. Holtzman, G. Flaggs, K. S. Keegan, A. DeMaggio, J. C. Ford, M. Hoekstra, and A. M. Carr.** 1996. The Schizosaccharomyces pombe rad3 checkpoint gene. EMBO J. **15:**6641–6651.
7. **Blasina, A., B. D. Price, G. A. Turenne, and C. H. McGowan.** 1999. Caffeine inhibits the checkpoint kinase ATM. Curr. Biol. **9:**1135–1138.
8. **Bouvard, V., T. Zaitchouk, M. Vacher, A. Duthu, M. Canivet, C. Choisy-Rossi, M. Nieruchalski, and E. May.** 2000. Tissue and cell-specific expression of the p53-target genes: bax, fas, mdm2 and waf1/p21, before and following ionising irradiation in mice. Oncogene **19:**649–660.
9. **Canman, C. E., D. S. Lim, K. A. Cimprich, Y. Taya, K. Tamai, K. Sakaguchi, E. Appella, M. B. Kastan, and J. D. Siliciano.** 1998. Activation of the ATM kinase by ionizing radiation and phosphorylation of p53. Science **281:**1677–1679.
10. **Chaturvedi, P., W. K. Eng, Y. Zhu, M. R. Mattern, R. Mishra, M. R. Hurle, X. Zhang, R. S. Annan, Q. Lu, L. F. Faucette, G. F. Scott, X. Li, S. A. Carr, R. K. Johnson, J. D. Winkler, and B. B. Zhou.** 1999. Mammalian Chk2 is a downstream effector of the ATM-dependent DNA damage checkpoint pathway. Oncogene **18:**4047–4054.
11. **Chehab, N. H., A. Malikzay, M. Appel, and T. D. Halazonetis.** 2000. Chk2/hCds1 functions as a DNA damage checkpoint in G(1) by stabilizing p53. Genes Dev. **14:**278–288.
12. **Chehab, N. H., A. Malikzay, E. S. Stavridi, and T. D. Halazonetis.** 1999. Phosphorylation of Ser-20 mediates stabilization of human p53 in response to DNA damage. Proc. Natl. Acad. Sci. USA **96:**13777–13782.
13. **Cimprich, K. A., T. B. Shin, C. T. Keith, and S. L. Schreiber.** 1996. cDNA cloning and gene mapping of a candidate human cell cycle checkpoint protein. Proc. Natl. Acad. Sci. USA **93:**2850–2855.
14. **Cliby, W. A., C. J. Roberts, K. A. Cimprich, C. M. Stringer, J. R. Lamb, S. L. Schreiber, and S. H. Friend.** 1998. Overexpression of a kinase-inactive ATR protein causes sensitivity to DNA-damaging agents and defects in cell cycle checkpoints. EMBO J. **17:**159–169.
15. **Corominas, M., J. Leon, H. Kamino, M. Cruz-Alvarez, S. C. Novick, and A. Pellicer.** 1991. Oncogene involvement in tumor regression: H-ras activation in the rabbit keratoacanthoma model. Oncogene **6:**645–651.
16. **Cortez, D., S. Guntuku, J. Qin, and S. J. Elledge.** 2001. ATR and ATRIP: partners in checkpoint signaling. Science **294:**1713–1716.
17. **Cortez, D., Y. Wang, J. Qin, and S. J. Elledge.** 1999. Requirement of ATM-dependent phosphorylation of brca1 in the DNA damage response to double-strand breaks. Science **286:**1162–1166.
18. **Deng, C., P. Zhang, J. W. Harper, S. J. Elledge, and P. Leder.** 1995. Mice lacking p21CIP1/WAF1 undergo normal development, but are defective in G1 checkpoint control. Cell **82:**675–684.
19. **el-Deiry, W. S.** 1998. Regulation of p53 downstream genes. Semin. Cancer Biol. **8:**345–357.
20. **Elledge, S. J.** 1996. Cell cycle checkpoints: preventing an identity crisis. Science **274:**1664–1672.
21. **Elson, A., Y. Wang, C. J. Daugherty, C. C. Morton, F. Zhou, J. Campos-Torres, and P. Leder.** 1996. Pleiotropic defects in ataxia-telangiectasia protein-deficient mice. Proc. Natl. Acad. Sci. USA **93:**13084–13089.
22. **Falck, J., N. Mailand, R. G. Syljuasen, J. Bartek, and J. Lukas.** 2001. The ATM-Chk2-Cdc25A checkpoint pathway guards against radioresistant DNA synthesis. Nature **410:**842–847.
23. **Giaccia, A. J., and M. B. Kastan.** 1998. The complexity of p53 modulation: emerging patterns from divergent signals. Genes Dev. **12:**2973–2983.
24. **Herzog, K. H., M. J. Chong, M. Kapsetaki, J. I. Morgan, and P. J. McKinnon.** 1998. Requirement for Atm in ionizing radiation-induced cell death in the developing central nervous system. Science **280:**1089–1091.
25. **Higashimoto, Y., S. Saito, X. H. Tong, A. Hong, K. Sakaguchi, E. Appella, and C. W. Anderson.** 2000. Human p53 is phosphorylated on serines 6 and 9 in response to DNA damage-inducing agents. J. Biol. Chem. **275:**23199–23203.
26. **Hirao, A., Y. Y. Kong, S. Matsuoka, A. Wakeham, J. Ruland, H. Yoshida, D. Liu, S. J. Elledge, and T. W. Mak.** 2000. DNA damage-induced activation of p53 by the checkpoint kinase Chk2. Science **287:**1824–1827.
27. **Jaspers, N. G., R. A. Gatti, C. Baan, P. C. Linssen, and D. Bootsma.** 1988. Genetic complementation analysis of ataxia telangiectasia and Nijmegen breakage syndrome: a survey of 50 patients. Cytogenet. Cell Genet. **49:**259–263.
28. **Lambert, P. F., F. Kashanchi, M. F. Radonovich, R. Shiekhattar, and J. N. Brady.** 1998. Phosphorylation of p53 serine 15 increases interaction with CBP. J. Biol. Chem. **273:**33048–33053.
29. **Levine, A. J.** 1997. p53, the cellular gatekeeper for growth and division. Cell **88:**323–331.
30. **Liao, M. J., and T. Van Dyke.** 1999. Critical role for Atm in suppressing V(D)J recombination-driven thymic lymphoma. Genes Dev. **13:**1246–1250.
31. **Lim, D. S., S. T. Kim, B. Xu, R. S. Maser, J. Lin, J. H. Petrini, and M. B. Kastan.** 2000. ATM phosphorylates p95/nbs1 in an S-phase checkpoint pathway. Nature **404:**613–617.
32. **Lindsten, T., A. J. Ross, A. King, W. X. Zong, J. C. Rathmell, H. A. Shiels, E. Ulrich, K. G. Waymire, P. Mahar, K. Frauwirth, Y. Chen, M. Wei, V. M. Eng, D. M. Adelman, M. C. Simon, A. Ma, J. A. Golden, G. Evan, S. J. Korsmeyer, G. R. MacGregor, and C. B. Thompson.** 2000. The combined functions of proapoptotic Bcl-2 family members bak and bax are essential for normal development of multiple tissues. Mol. Cell **6:**1389–1399.
33. **Lomaga, M. A., J. T. Henderson, A. J. Elia, J. Robertson, R. S. Noyce, W. C. Yeh, and T. W. Mak.** 2000. Tumor necrosis factor receptor-associated factor 6 (TRAF6) deficiency results in exencephaly and is required for apoptosis within the developing CNS. J. Neurosci. **20:**7384–7393.
34. **Matsuoka, S., M. Huang, and S. J. Elledge.** 1998. Linkage of ATM to cell cycle regulation by the Chk2 protein kinase. Science **282:**1893–1897.
35. **Matsuoka, S., G. Rotman, A. Ogawa, Y. Shiloh, K. Tamai, and S. J. Elledge.** 2000. Ataxia telangiectasia-mutated phosphorylates Chk2 in vivo and in vitro. Proc. Natl. Acad. Sci. USA **97:**10389–10394.
36. **Melchionna, R., X. B. Chen, A. Blasina, and C. H. McGowan.** 2000. Threonine 68 is required for radiation-induced phosphorylation and activation of Cds1. Nat. Cell Biol. **2:**762–765.
37. **Meyn, M. S.** 1995. Ataxia-telangiectasia and cellular responses to DNA damage. Cancer Res. **55:**5991–6001.
38. **Oda, K., H. Arakawa, T. Tanaka, K. Matsuda, C. Tanikawa, T. Mori, H. Nishimori, K. Tamai, T. Tokino, Y. Nakamura, and Y. Taya.** 2000. p53AIP1, a potential mediator of p53-dependent apoptosis, and its regulation by Ser-46-phosphorylated p53. Cell **102:**849–862.
39. **Prives, C.** 1998. Signaling to p53: breaking the MDM2-p53 circuit. Cell **95:**5–8.
40. **Quintanilla, M., K. Brown, M. Ramsden, and A. Balmain.** 1986. Carcinogen-

specific mutation and amplification of Ha-ras during mouse skin carcinogenesis. Nature **322:**78–80.
41. **Sakaguchi, K., J. E. Herrera, S. Saito, T. Miki, M. Bustin, A. Vassilev, C. W. Anderson, and E. Appella.** 1998. DNA damage activates p53 through a phosphorylation-acetylation cascade. Genes Dev. **12:**2831–2841.
42. **Shieh, S. Y., J. Ahn, K. Tamai, Y. Taya, and C. Prives.** 2000. The human homologs of checkpoint kinases Chk1 and Cds1 (Chk2) phosphorylate p53 at multiple DNA damage-inducible sites. Genes Dev. **14:**289–300.
43. **Shieh, S. Y., M. Ikeda, Y. Taya, and C. Prives.** 1997. DNA damage-induced phosphorylation of p53 alleviates inhibition by MDM2. Cell **91:**325–334.
44. **Shieh, S. Y., Y. Taya, and C. Prives.** 1999. DNA damage-inducible phosphorylation of p53 at N-terminal sites including a novel site, Ser20, requires tetramerization. EMBO J. **18:**1815–1823.
45. **Shiloh, Y.** 1995. Ataxia-telangiectasia: closer to unraveling the mystery. Eur. J. Hum. Genet. **3:**116–138.
46. **Shiloh, Y.** 2001. ATM and ATR: networking cellular responses to DNA damage. Curr. Opin. Genet. Dev. **11:**71–77.
47. **Siliciano, J. D., C. E. Canman, Y. Taya, K. Sakaguchi, E. Appella, and M. B. Kastan.** 1997. DNA damage induces phosphorylation of the amino terminus of p53. Genes Dev. **11:**3471–3481.
48. **Song, S., and P. F. Lambert.** 1999. Different responses of epidermal and hair follicular cells to radiation correlate with distinct patterns of p53 and p21 induction. Am. J. Pathol. **155:**1121–1127.
49. **Tibbetts, R. S., K. M. Brumbaugh, J. M. Williams, J. N. Sarkaria, W. A. Cliby, S. Y. Shieh, Y. Taya, C. Prives, and R. T. Abraham.** 1999. A role for ATR in the DNA damage-induced phosphorylation of p53. Genes Dev. **13:**152–157.
50. **Varley, J. M., G. McGown, M. Thorncroft, M. F. Santibanez-Koref, A. M. Kelsey, K. J. Tricker, D. G. Evans, and J. M. Birch.** 1997. Germ-line mutations of TP53 in Li-Fraumeni families: an extended study of 39 families. Cancer Res. **57:**3245–3252.
51. **Westphal, C. H., S. Rowan, C. Schmaltz, A. Elson, D. E. Fisher, and P. Leder.** 1997. atm and p53 cooperate in apoptosis and suppression of tumorigenesis, but not in resistance to acute radiation toxicity. Nat. Genet. **16:**397–401.
52. **Xu, Y., T. Ashley, E. E. Brainerd, R. T. Bronson, M. S. Meyn, and D. Baltimore.** 1996. Targeted disruption of ATM leads to growth retardation, chromosomal fragmentation during meiosis, immune defects, and thymic lymphoma. Genes Dev. **10:**2411–2422.
53. **Xu, Y., and D. Baltimore.** 1996. Dual roles of ATM in the cellular response to radiation and in cell growth control. Genes Dev. **10:**2401–2410.
54. **Zhao, R., K. Gish, M. Murphy, Y. Yin, D. Notterman, W. H. Hoffman, E. Tom, D. H. Mack, and A. J. Levine.** 2000. Analysis of p53-regulated gene expression patterns using oligonucleotide arrays. Genes Dev. **14:**981–993.
55. **Zhou, B. B., P. Chaturvedi, K. Spring, S. P. Scott, R. A. Johanson, R. Mishra, M. R. Mattern, J. D. Winkler, and K. K. Khanna.** 2000. Caffeine abolishes the mammalian G(2)/M DNA damage checkpoint by inhibiting ataxia-telangiectasia-mutated kinase activity. J. Biol. Chem. **275:**10342–10348.
56. **Zhou, B. B., and S. J. Elledge.** 2000. The DNA damage response: putting checkpoints in perspective. Nature **408:**433–439.